A Comparison Study between 3-D CFD and Experimental Data of Butterfly Valve Coefficients

دراسة مقارنة بين الحسابات العددية ثلاثية الأبعاد والعملية لمعاملات صمام الفراشة

Mohammed M. Said[a,1], Hossam S.S. AbdelMeguid[b,2], and Lotfy H. Rabie[b,3]

[a] GUPCO - Gulf of Suez Petroleum Co., 270 Palestine St. 4th Sector, New Maadi, Maadi, Cairo, Egypt.
[b] Mechanical Power Engineering Department, Faculty of Engineering, Mansoura University, El-Mansoura 35516, Egypt
[1] Email: saidmm@gupco.net, Tel.: +201092647247
[2] Email: hssaleh@mans.edu.eg, Tel.: +201066464712
[3] Email: lotfyrs@hotmail.com, Tel.: +201000076754

ملخص

لقد أصبح استخدام الحسابات العددية في إختبار صمامات التحكم من الأمور المهمة في التطبيقات الصناعية. ويعتبر برنامج Fluent6.3 واحداً من البرامج المستخدمة في الحلول الرقمية للعديد من المشكلات الهندسية. ولقد إزدادت الحاجة لمعرفة خصائص السريان حول صمام الفراشة لإستخداماته الصناعية الواسعة. وقبل الشروع في الحسابات تم عمل إختبار التأكدية للبناء الرقمي والذي تم إنشائه ببرنامج Gambit2.4 لصمام فراشة 2 بوصة ثلاثى الأبعاد كما تم إختبار توزيع سرعة المائع عددياً ووجد أن توزيع السرعة تتفق مع قانون الأس 7 لتوزيع السرعة خلال الأنابيب. بعد فحص معامل فقد الضغط عددياً عند الزوايا من 30° إلى 90° وبطريقتين مختلفتين: الأولى عند سرعات مختلفة للمائع والأخرى عند سرعة ثابتة وجد أن المفاقيد الهيدروليكية لا تعتمد على السرعة ولكنها تعتمد على التغير في فتحة الصمام في علاقة أسية وهذا يتفق مع ما نُشر في [1]. كما تم حساب معامل سريان الصمام ومقارنته ببيانات المُصَنع فوجد تقارباً كبيراً بينهما مع حيود عند الزاويتين 80° و90° . كما تم حساب معامل العزم للصمام ووجد أن أقصى معامل عزم هيدروليكي عند زواية 70° وهذا يتفق مع ما نُشر في [٢]. كما تم إثبات أن قوى العزم الهيدروليكية تتعاظم عند 70° كما تتعاظم المفاقيد الهيدروليكية للفتحات أقل من 40° وهذا الذى يفسر قيود تشغيل الصمام عند زوايا أقل من 40° وعند زوايا أكبرمن 70°. وأخيراً رغم ما يتطلبه قُرص الصمام من تعديل للتغلب على الإضطرابات الحادثه لسريان المائع خلاله عند الزوايا من 70° إلى 90° إلا أنه لا يحتاج لأية تعديلات من ناحية متطلبات العزم الهيدروليكي عند أية زاوية. لذلك يمكن استخدام الحسابات الرقمية بنجاح للوصول لأفضل متطلبات التصميم لصمام الفراشة. وفي المستقبل نأمل في دراسة تأثير ظاهرة التكهف على معاملات الأداء لهذا الصمام.

1. Abstract

Computational fluid dynamics (CFD) enables scientists and engineers to perform ‘numerical experiments’ (i.e., computer simulations) in a ‘virtual flow laboratory’. Numerical simulation permits valve manufacture to determine valve sizing coefficients and to solve problems involving valves fluid flow. Valve designer via CFD could identify and eliminate valve flow problems before starting the manufacturing step. This technique is less costly alternative to determine the flow coefficients based on CFD calculations. Butterfly valves are versatile components widely used in hydraulic systems as shutoff and throttling valves. In this study, a comprehensive 3D simulation study for 2" (50 DN STC model) butterfly valve is conducted to establish a trusted and a calibrated numerical solution model after comparing with experimental data. The goal of this study is to verify and validate CFD code to obtain reasonable results for control valve coefficients calculation. The steady and incompressible Navier-Stokes equations are solved numerically to predict the flow behavior and compute the pressure loss, flow, and torque coefficients.

Keywords: CFD, control valve, butterfly valve, valve coefficients.

Received: 2 July, 2014 - Revised: 11 August, 2014 - Accepted: 24 September, 2014

2. Introduction

CFD validation weight increases with time. Researchers use numerical techniques to solve problems involving fluid flow, heat and mass transfer, chemical reactions, and related complex phenomena. Most of the commercial CFD solvers are based on the finite volume method in which the continuous flow domain is replaced by a discrete one using grid points. Fluent 6.3 is one of these CFD solvers including several models to solve incompressible, steady and turbulent flow at these grid points.

Using CFD in control valves design to predict the fluid flow and pressure distribution is attractive to industry since it is less costly than valve experimental tests. Butterfly valve and its actuator should be mutually compatible to withstand the torque that is applied during its service of operation. On that basis, to select the economical actuator for a control valve, the foremost effective factor is the torque required to operate the valve [3].

Butterfly control valves are sized according to the valve coefficients at different disk angles (α). Misconception in sizing butterfly valves can destroy the flow continuity and change the physical performance. In many cases, it results in undesirable effects such as intensive noise and vibration which can limit the life expectancy of the valve. Therefore, it is very important to know in which conditions the butterfly valves exhibit high performance, i.e., minimum pressure drop and large flow coefficient.

CFD provides local information of all the variables as, pressure and velocity around the control valve disk. In many instances, the determination of control valve coefficients: pressure drop, flow, cavitation, and torque coefficients, as a function of valve disk angle is essential to compare valve performances for specific application. On that basis, these coefficients are the basic step to optimize the selection among different manufactures. Butterfly valve is a type of flow control device, which is widely used in industry application to regulate the fluid flow in pipelines. Studies on flow behavior inside these valves endeavor to optimize the valve design and selection. Jeon et al. [4] studied the performance of butterfly valve disk, and the flow characteristics using CFD. The results showed that the flow pattern associated with a double disk is more complex compared to a single disk type due to formation of recirculating eddies, at the rear of valve disk. Moreover, the results showed that valves hydrodynamic behavior and their dynamic torque coefficients were affected by the shape of the disk geometry. Vakili-Tahami et al. [5] studied numerically 1000 mm diameter butterfly valve using Cosmos FloWorks software. The results revealed that the valve disk surface roughness has an insignificant effect on the disk opening torque. Thanigavelmurugan et al. [6] employed CFD analysis to design the tortuous path and to study the flow field and performance of high pressure turbine bypass valve. The results showed that the valve performance is satisfactory with the operating conditions. Leutwyler and Dalton [7] utilized Fluent 6.0 to predict the pressure profile on the butterfly valve disk at angles 30°, 45°, and 60°. The numerical results depicted that for certain disk angles, significant fluctuations in the torque are present and cause severe vibrations to the piping system. Shirazi et al. [8] concluded the ball valve 3-order polynomial equation for the relation between the ball valve pressure loss coefficient and valve disk angle using CFD analysis. Sonawane et al. [9] studied the flow pattern of the globe valve using 3-D CFD simulations. The numerical results were used to estimate the valve flow coefficients at different flow rates and constant pressure drop across the valve. The results closely matched with the laboratory testing data. Wang et al. [10] studied the fluid flow properties in a large butterfly valve using fluid structure interaction (FSI) to determine whether it can work safely or not. The results of FSI suggested that large butterfly valve should

not be fixed at a low opening angle, and also the improvement of butterfly valve design is conducted in their study. Price [11] examined the effect of the pipeline length and valve closure time on the transient dynamic torque that was applied to butterfly valves. The results showed that there is a noticeably large increase in dynamic torque when the valve is being closed with long pipelines and short closure times. Morita et al. [12] examined in details the unsteady phenomena of steam valve in mid-opening position to understand the flow characteristics using CFD because the flow around the valve had a complex 3-D structure. The results confirmed that the CFD validity, as the unsteady phenomena that were observed and the unsteady region, amplitude and frequency agree well with those of experiment. Prema et al. [13] studied the design optimization using CFD for butterfly disk. The result showed that the flow coefficient increases by 56.8 % after redesigning the stem by the optimized design. The valve manufactures present their products with the valve coefficients which are the major target in the case of good sizing and selection process. Chern and Wang [14] investigated numerically and experimentally the fluid flow which was controlled by a full-port 1/4 turn valve with a V-port. It was observed that, the smaller the angle of a V-port, the more the pressure loss.

The present research aims to study numerically the pressure loss, torque and flow coefficients of butterfly valve at different disk angles (α) for different operating conditions. To establish a CFD model for the butterfly valve with the connected pipeline, Gambit 2.4 is employed to the 3D flow domain and generate the mesh. Numerical results are obtained by using Fluent 6.3 with applying the k-ε turbulence model to solve the RANS continuity and momentum equations. The pressure loss, torque and flow coefficients are calculated. The fluid flow field represented by velocity and pressure distributions for disk angles (α) 30° to 90° (fully-opened position) is also presented in this study.

3. Butterfly valve performance coefficients

The principal use of valve performance coefficients is to aid in the selection of appreciated valve size for specific application. All the pertinent sizing factors must be known at different valve disk angles (α). Butterfly valve performance coefficients include pressure loss, flow, and hydrodynamic torque coefficients. Whereas these values can usually be obtained experimentally, it is sometimes not possible to identify these coefficients experimentally. Another method wherein butterfly valve performance coefficients can be obtained is by using CFD.

3.1 Pressure loss coefficient

The pressure loss coefficient, k, is a dimensionless value commonly used to predict the minor head loss due to the presence of valve in fluid flow field. It is essential to obtain the valve pressure loss coefficient as a function of valve disk angle (α). Two different methods are used numerically to investigate the relation between the pressure loss coefficient and the disk angle:

- Fixed inlet velocity of 1.9 m/s and free discharge (atmospheric outlet pressure).
- Varying inlet velocity (i.e., varying Reynolds number) and fixed discharge pressure (0.69 barg) as listed in Table 1.

The pressure loss coefficient, k, can be calculated by:

$$k = \frac{\Delta P}{\frac{1}{2}\rho . U^2} \qquad (1)$$

Reynolds number = $\frac{U.d}{\nu}$

where

ΔP: Difference between inlet and outlet pressures (N/m^2)

ρ: Density (kg/m^3)

U: Average velocity (m/s)

d: Pipeline diameter (m)

ν: Kinematic viscosity (m^2/s)

Table 1 Reynolds number values with different angles.

α (°)	**30**	**40**	**50**	**60**	**70**	**80**	**90**
U (m/s)	3.8	6.8	11.1	12.8	17.7	25.0	27.5
Re x 10^4	1.4	2.6	4.2	4.8	6.7	9.4	10.4

3.2 Flow coefficient

The flow coefficient, Cv, is the volume (in US gallons) of water at 60° F that flow per minute through a valve with a pressure drop of 1 psi and can be calculated by:

$$Cv = \frac{Q}{\sqrt{\Delta P_{ISA}/\gamma}} \qquad (2)$$

where

Q: Flow rate (US gallons per minute)

ΔP_{ISA}: Pressure drop across the valve (2d and 6d) before and after the valve disk respectively (psi)

γ: Specific gravity of fluid (γ for water = 1)

Cv: Flow coefficient

The valve flow coefficient that compatible with SI units is A_v, which does not have a wide acceptance by the technical community. ΔP_{ISA} is measured according ISA standard for testing control valves. In this standard the upstream pressure measured from a pipe tap 2d before the valve and the downstream pressure from a pipe tap 6d after the valve. Eq. (2) ignores the pressure drop between these taps and the valve. Therefore, for maximum accuracy, ΔP_{ISA} should be superseded by ΔP_{NET} (is the pressure drop across the valve and close to the disk), as will be explained later. The numerically computed flow coefficients, as shown in Fig. 10 are compared with the manufacture flow coefficients that are listed in Table 2.

Table 2 Manufacture Cv values for 50DN STC model butterfly valve at different disk angles (α).

Size	**2″ (50 mm)**							
α (°)	20	30	40	50	60	70	80	90
Cv	8	9	18	28	55	72	110	135

3.3 Dynamic torque coefficient

The torque of butterfly valves is the turning force needed to rotate the valve disk or hold it in a certain position [15]. Torque coefficient, C_t, is a dimensionless value ,which depends on the valve disk shape, disk opening angle, valve type and the offset of valve stem with disk.

The dynamic torque coefficient is determined by involving the hydrodynamic torque, T_{dy} as given by:

$$T_{dy} = C_t . D^3 . \Delta P \qquad (3)$$

where

T_{dy} : Dynamic torque (N.m)

ΔP: Difference between inlet and outlet pressures (N/m^2)

D: Diameter of the valve disk (m)

C_t: Torque coefficient

Dynamic torque is a function of the diameter to the third power; therefore, it becomes increasingly more significant as valve diameters increase. The resulting force vector components in Cartesian coordinate for all grid nodes are summed after multiplied by the corresponding arms to calculate the hydrodynamic torque.

The obtained numerical results of torque coefficient at different disk angles are compared with the results of Henderson et al. [2].

4. CFD model

This section presents the valve and connected pipes dimensions and geometry, governing equations, boundary conditions and the CFD solving model.

4.1 Physical model description

Stonetown butterfly valve, STC type, DN 50, class #150 is shown in Fig. 1. The disk diameter (D) is 49 mm with thickness 3.175 mm. The disk geometry is a circular plate connected with two semicircular hubs 12.7 mm radius. The hubs are aligned parallel to the valve stem

upstream and downstream the valve disk. The flow volume consists of the valve disk inserted in the pipe with 2d length upstream the valve and 6d downstream the valve. These dimensions are shown schematically in Fig. 2, this layout choice complies with [13, 14, 16].

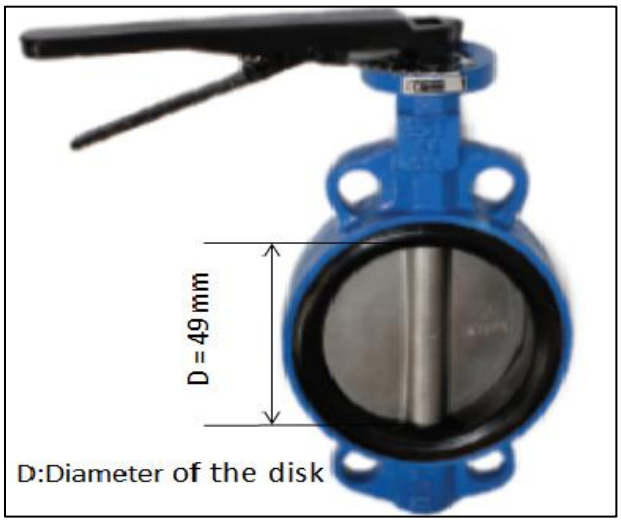

Fig. 1 STC butterfly valve

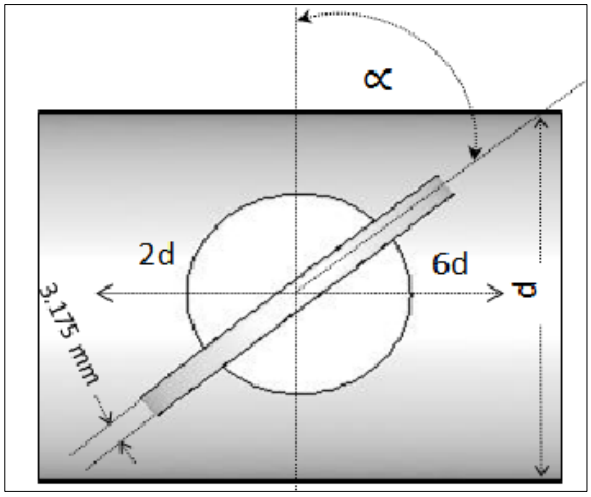

Fig. 2 STC butterfly valve volume flow domain drawn by Gambit 2.4 (This drawing is not to scale).

4.2 Mathematical model

The governing equations are the Navier-Stokes and continuity equations. The equations for steady state, incompressible Newtonian fluid are described by Eqs. (4), (5), and (6).

$$\rho \frac{\partial}{\partial x_j}(u_j u_i) = -\frac{\partial P}{\partial x_i} + \frac{\partial}{\partial x_j}(2\mu S_{ij}) \qquad (4)$$

$$\frac{\partial u_i}{\partial x_i} = 0 \qquad (5)$$

where $i, j, k = 1\sim3$, and u_i, u_j, u_k are the velocity vectors in the three perpendicular Cartesian coordinates x_i, x_j, x_k. S_{ij} is the strain–rate tensor given by:

$$S_{ij} = \frac{1}{2}\left(\frac{\partial u_i}{\partial x_j} + \frac{\partial u_j}{\partial x_i}\right) \qquad (6)$$

One approach was used to solve Navier-Stokes equations includes focusing on the effects of turbulence on mean flow properties by using what is called Reynolds-Averaged Navier-Stokes (RANS). The RANS is represented by:

$$\rho \frac{\partial}{\partial x_j}(U_i U_j) = -\frac{\partial P}{\partial x_i} + \frac{\partial}{\partial x_j}(2\mu S_{ij} - \rho\overline{u_i' u_j'}) \qquad (7)$$

where

U_i and U_j: The time-averaged value of the velocity vectors in the two perpendicular Cartesian coordinates x_i, x_j.

u_i' and u_j': The fluctuating velocity is in two perpendicular Cartesian coordinates x_i, x_j.

$\frac{\partial}{\partial x_j}(\overline{u_i' u_j'})$: Reynolds stresses term.

In order to compute the turbulent flows with Eq. (7), it is necessary to develop the turbulence model to predict the Reynolds stresses. One of the most common turbulence models is the k-ε model which is used to solve the RANS equations to predict turbulent flows for 3D butterfly valve. The standard k-ε turbulence model is selected from different models in Fluent 6.3 due to its accuracy, free from the complex and non-linear damping functions that are required for the other models. Huang and Kim [17] utilized Fluent to simulate turbulent flows in a butterfly valve, in which the k-ε model was employed for turbulence consideration. The model is a

transport equation for the kinetic energy (k) and its dissipation rate (ε) as described by Eqs. (8) and (9).

Changes of k (kinetic energy)

$$U_j \frac{\partial k}{\partial x_j} = \tau_{ij} \frac{\partial U_i}{\partial x_j} - \varepsilon + \frac{\partial}{\partial x_j}\left(\left[\nu + \frac{\nu_T}{\sigma_k}\right]\frac{\partial k}{\partial x_j}\right) \quad (8)$$

Changes of ε (dissipation rate)

$$U_j \frac{\partial \varepsilon}{\partial x_j} = C_{\varepsilon 1} \frac{\varepsilon}{k} \tau_{ij} \frac{\partial U_i}{\partial x_j} - C_{\varepsilon 2} \frac{\varepsilon^2}{k} + \frac{\partial}{\partial x_j}\left(\left[\nu + \frac{\nu_T}{\sigma_\varepsilon}\right]\frac{\partial \varepsilon}{\partial x_j}\right) \quad (9)$$

where

$$\nu_T = c_\mu \frac{k^2}{\varepsilon} \quad (10)$$

The constants values are [18]:

c_μ=0.09, $C_{\varepsilon 1}$=1.44, $C_{\varepsilon 2}$=1.92, σ_k=1, σ_ε=1.3

4.3 Mesh generation

Basically, there are three main stages in CFD methodology which are typically followed in this study. These stages are :Pre-processing, Solving and Post-processing. The studied flow volume including the valve disk and the connected pipes is meshed via Gambit 2.4. The generated mesh has been repeated for different mesh types and sizes, the best efficient mesh method for converging solution is executed using unstructured (tetrahedral) and T-grid type. The final meshes are generated for seven different disk angles from 30° to 90° with incremental step of 10°. An illustration of the geometry and mesh are shown in Figs. 2 and 3 with locally re-fined numerical grid of high density ranges from $0.8x10^6$ to $1.2x10^6$ elements. The model previously described is implemented directly into Fluent 6.3. Partial differential equations are discretized into a system of algebraic equations and these algebraic equations are then solved numerically over each elemental discrete volume.

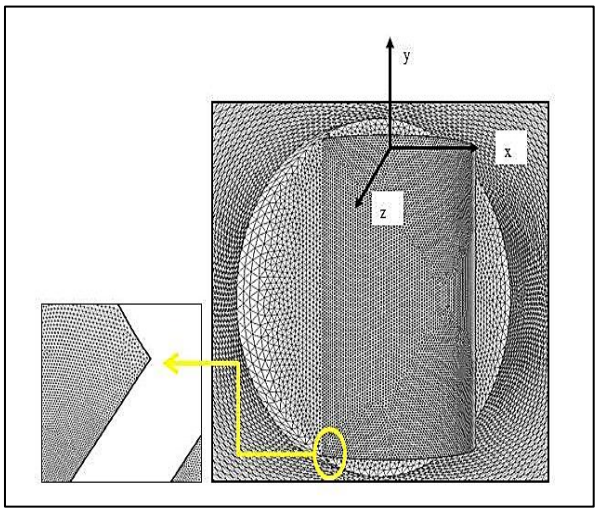

Fig. 3 Mesh for valve disk angle of 40°.

4.4 Boundary conditions

A large source of uncertainty in CFD modeling can result from poor representation of boundary conditions, particularly, the inlet [7]. It is very important to specify the proper boundary conditions in order to have a well-defined problem.

In 3D, boundaries are surfaces that completely surround and define a region. The defined boundary conditions of the outlet pressure, the inlet velocity, k_{wall}, and ε_{wall} for the disk surfaces and the pipe walls are varnished in Table 3. At solid boundaries, the no-slip condition is applied for all disk angles.

Table 3 Fluent 6.3 fixed entries and boundary conditions data

Variables	Value
Inlet velocity	1.9 m/s
Outlet pressure	0 barg
Turbulence intensity (I)	4 %
k_{wall}	0
ε_{wall}	0
Density	998.2 kg/m³
Viscosity	$1.13x\ 10^{-6}$m²/s
Hydraulic diameter	0.049 m
Reynolds no.	$8.2x10^4$

5. Results and discussion

The target from the numerical simulation is to compute the fluid flow properties to obtain valve performance curves for valve disk angles from α=30° to 90° with incremental step of 10°. The calculated valve coefficients are analyzed in this section. Furthermore, constructing validity and accuracy degree of numerical results are also discussed. HP G62 PC laptop with Intel processor core (i5) CPU M 460 @ 2.53GHz and memory of 3 GB RAM is used to perform the simulations. Despite there are differences between the meshes of the executed cases for each disk angle, the mean run time is about 8 hours.

5.1 Results validation and accuracy

Mesh independence test

Simulated engineering cases via CFD, especially complex cases, are prone to errors from different sides. The most arising challenging side is the meshing phase. Mesh resolution has a strong influence on the quality of the numerical results and computational time required. Sometimes, it takes a lot of time efforts and engineering skills to obtain the validated solution. Mesh independence test is performed for 3-D butterfly valve at 60° disk angle. The repetition of the calculation using Fluent 6.3 with a higher mesh resolution until a good degree of accurate results is achieved. The converging criteria is established when the numerical solutions obtained for the inlet pressure on different grids agrees to within a level of tolerance of 0.001. The number of mesh elements is increased gradually with avoiding skewed elements and aspect ratio violation till defining the number of elements where the solution is independent on the mesh density. As illustrated in Table 4, and after performing four trials, the number of grid points is increased, the error in the numerical solution decreases. The result obtained for cell resolution around $1.188x10^6$ is adopted in the present study. A mesh of higher density is generated close to and around the valve disk.

Table 4 Mesh independence test for disk angle of 60^o

No.	Mesh dependence test (60°)			Inlet pressure (psig)	Error (%)	Time (Hour)
	No. of cells	No. of faces	No. of nodes			
1	275,034	581,397	62,066	0.814	-	4
2	533,055	1,111,892	112,717	0.753	8	6
3	1,188,539	2,476,541	249,793	0.737	2	8
4	1,774,814	3,703,369	375,994	0.737	0.1	10

The flow coefficient, Cv, is calculated from the numerical results of different mesh resolutions. As depicted in Fig. 4, the value of Cv for trials 3 and 4 are indistinguishable.

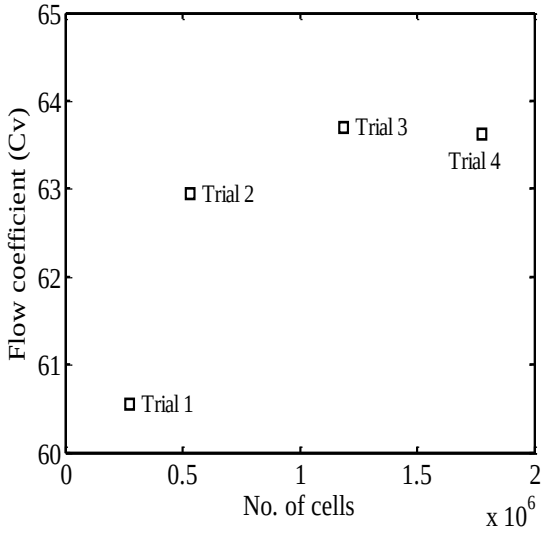

Fig. 4 Cv variation with mesh density

Velocity profile

The numerical results of the dimensionless velocity profile for fully-opened valve ($\alpha = 90^o$) are shown in Fig. 5. This result is used to identify the turbulent exponent n in Eq. (11) which is derived for the turbulent flow model [18].

$$\frac{U}{U_m} = \left(1 - \frac{r}{R}\right)^{\frac{1}{n}} \qquad (11)$$

Where

U_m: Maximum centerline velocity (m/s)

R: Pipeline radius (m)

r: Distance from the centerline (m)

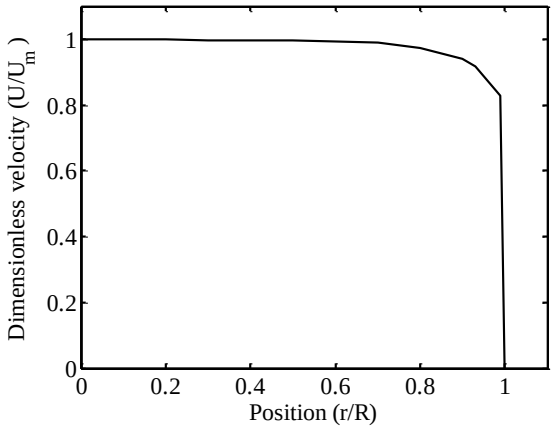

Fig. 5 Velocity profile for fully-opened position.

The value of n increases with increasing Reynolds number. The typical value of n ranges from 6 to 10 for turbulent flows. Henderson et al. [2] determined n from CFD analysis for a butterfly valve used in Hydro-electric power scheme as 10.5 and 11.4, but the value of n equal to 7 generally approximates many flows in practice. This value is giving rise to the term one-seventh power-law velocity profile. In this study, the average value of n is obtained from numerical results of the velocity at outlet zone. The value of n is found to be 8.6, which agrees with fully-developed turbulent flow.

5.2 Total pressure

Figure 6.a illustrates the numerical results of the total pressure ratio $\frac{P}{P_M}$ (normal pressure relative to maximum pressure) for the side view visualization of the flow field around the valve disk and along the pipe line for different disk angles. For disk angles smaller than 70^o ($\alpha < 70^o$), there are high pressure drops across the valve disk. Whereas, for larger angles ($\alpha > 70^o$), a relatively small pressure drop is observed. The pressure drop at disk angle of 80° and 90° is hardly distinguished. Therefore, the operation of butterfly valve is restricted to disk angle of 80°. For the disk angles 30° and 40°, the degree and extent of the formulated eddy zones behind the disk escalate while diminish gradually with larger disk angles.

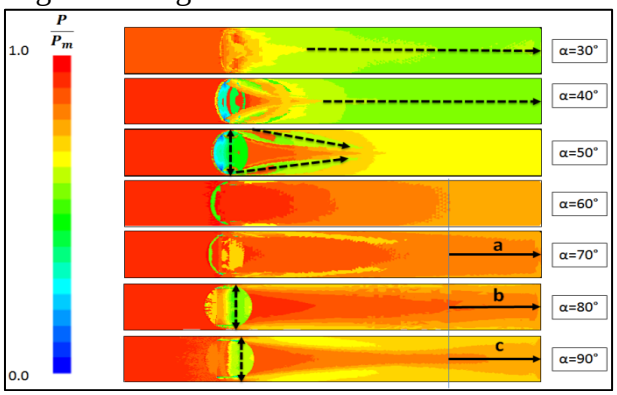

Fig. 6.a Side view for pressure profiles from angle 30° to 90°.

In the current numerical study, the outlet pressure boundary condition is set at atmospheric condition (free discharging case), which enhancing the existing of valve cavitation. The cavitation flow condition zones are formed horizontally downstream the valve disk at angles 30° and 40° and diagonally behind the valve at angle 50°, while they dominate vertically around the valve disk at angles 80° and 90°. These zones are represented by dashed arrow lines are shown schematically in Fig. 6.a. The downstream length of 6d is enough length to cover fully turbulent region for disk angle ranges from 30° to 60°. However, this is not yield for disk angle ranges from 70° to 90°, which are represented by arrow lines a, b, and c in Fig. 6.a. This observation concords with what was published by ISA. In cavitation circumstances, the downstream pressure of the control valve with a Cv/d^2 greater than 20 may not be fully recovered at the distance of 6d [16].

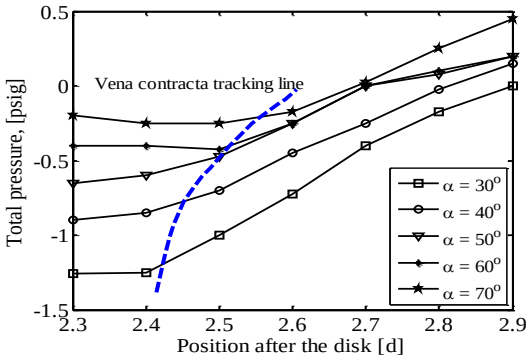

Fig. 6.b Pressure recovery curves 2d after the valve disk for angles 30° to 70°.

In Fig. 6.b, the pressure recovery from the valve centerline extended to 2d downstream the valve disk and along the pipe mid-line for disk angle ranges from 30° to 70°. It can be noticed that the pressure decreases as the fluid passes through the valve Vena contracta and then the pressure is partially recovered as the fluid enters the downstream pipe area. As depicted in Fig. 6.b, the point of lowest pressure (i.e., Vena contracta) lies behind the valve disk and moves far away the valve disk with increasing the valve disk angle. Furthermore, after 1d distance downstream the valve disk centerline, the pressure gradient along the perpendicular axis to the valve stem has a constant value, i.e., $(\frac{\partial p}{\partial x} = c)$.

5.3 Velocity magnitude

The butterfly valve is a quarter turn type which specifies a high recovery valve. The flow passing the valve at certain disk angle is divided between convergence-divergence pass at one disk side and to divergence-convergence pass in the other side. On that basis, the un-symmetry flow condition occurs around the valve disk as indicated in Fig. 7.a by dashed arrows at angle 50°, where $\frac{U}{U_m}$ is the normal maximum velocity relative to the maximum velocity.

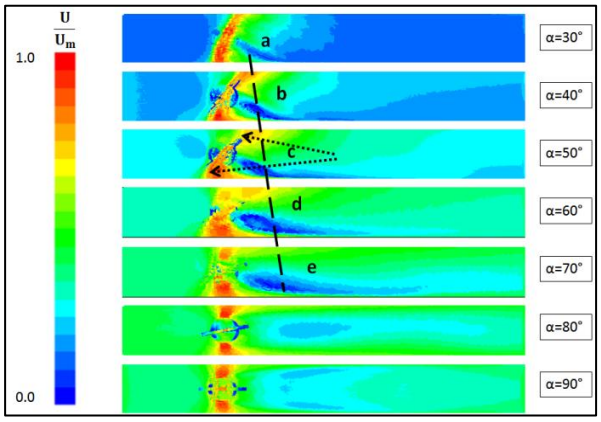

Fig. 7.a Top view for velocity profiles for different disk angles.

The extensive un-symmetry occurs at disk angles lower than 70^o ($\alpha \leq 70^o$), while a complete symmetry is found at disk angles of 80° and 90°. A moving and growing separation zone behind the valve as going from disk angle 30° has disappeared at disk angles 80° and 90°. This is depicted by the diagonal dashed line extended downstream the valve disk. The zone flows away from the disk wall instead of flowing along the wall and is presented by points a, b, c, d, and e. Turbulence kinetic energy from valve centerline to 2d after the valve disk for 30° to 70° angles is depicted in Fig. 7.b. Turbulence kinetic energy diminishes gradually from 30° toward large disk angle 70°, but between angles 40° and 50° there is a distinct rapid overshot value. This observation suggests that, for flow free of turbulence, the butterfly valve throttling below 40° is not recommended. This result concords with the finding of Ibrahim et al. [19]. They concluded that, the flow turbulence is more significant at valve angle of 35° and its intensity increases with small disk angles.

In Fig. 7.b, turbulence peaks occur near the disk wall between (2.5d and 2.6d) from pipe inlet behind the valve disk, and the peak value is shifted away in flow direction for large disk angles.

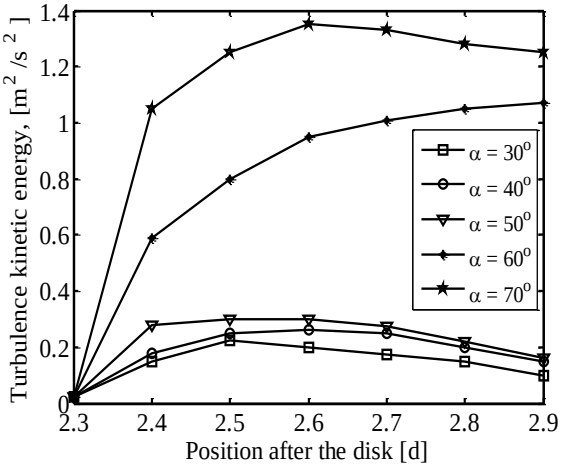

Fig. 7.b Turbulence kinetic energy curves 2d after the valve disk for different disk angles

5.4 Turbulence intensity

The results presented in Fig. 8 show that, the degree of turbulence depends on the valve disk angle, where $\frac{I}{I_m}$ is the

turbulence intensity relative to the maximum turbulence intensity. At small disk angles ranging from 30º to 50º, there is an escalated turbulence associated with the valve disk, and is enveloped by dash lines. While the turbulence decreases at large disk angles ranging from 70º to 90º, and is illustrated by dashed arrows.

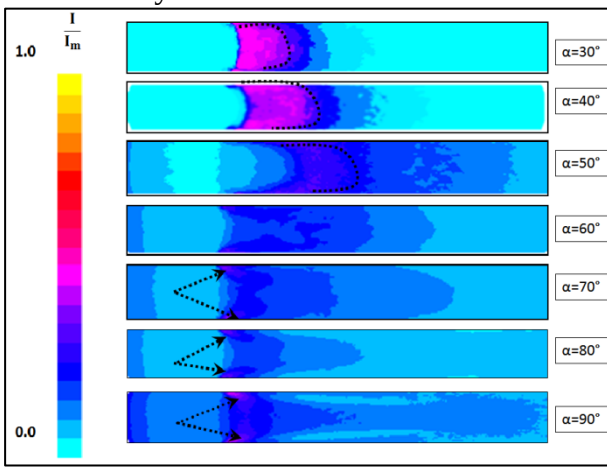

Fig. 8 Side view for turbulence intensity from angle 30° to 90°.

The growing up turbulence areas at large disk angles is due to existence of disk hub. However, the distinct limiting disk angle is 60º which is not subjected to any turbulence. Therefore, the disk geometry design may need adaptation to reduce the turbulence and to avoid flow disturbance that is affected by hub existence.

5.5 Pressure loss coefficient

The two criteria described in section 3.1 are used to investigate the relation between the pressure loss coefficient and the disk angle. The results are illustrated in Fig. 9, and are compared with the published results in Sandalci et al. [1]. The results show that there is no distinguishing between the two scenarios and also with Sandalci et al. [1]. The error is too small between exponential Eqs. (12-14). The pressure loss coefficient only depends on the valve geometry. Although increasing Reynolds number with large valve opening, the pressure loss coefficient tends to decrease, so the variation of the disk angle position has the major effect on the pressure loss coefficient, which agrees with Sandalci et al. [1].

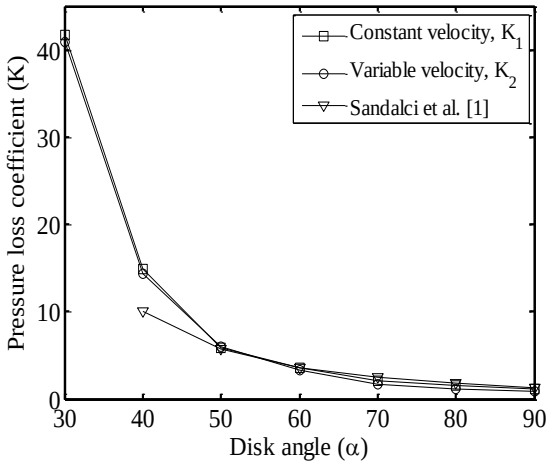

Fig. 9 The effect of the disk angle on the pressure loss coefficient.

From the numerical results of constant flow velocity method, a relation between pressure loss coefficient ζ_1 and disk angle (α) is given by:

$$\zeta_1 = 5 \times 10^6 \alpha^{-3.45}, \quad R^2 = 0.9912 \qquad (12)$$

The numerical results of variable flow velocity gives a relation between pressure loss coefficient ζ_2 and disk angle (α) as:

$$\zeta_2 = 8 \times 10^6 \alpha^{-3.65}, \quad R^2 = 0.998 \qquad (13)$$

Sandalci et al. [1] concluded that the pressure loss coefficient is independent of Reynolds number and its variation with the opening angle is given by:

$$K_{Sand.} = 1.074 \times 10^5 \, \alpha^{-2.514} \qquad (14)$$

which is very close to the obtained results as depicted in Fig. 9.

5.6 Flow coefficient

The numerically computed ISA pressure drop, ΔP_{ISA}, is the pressure difference between 2d and 6d upstream and downstream the valve, respectively. However, the net pressure drop, ΔP_{NET}, is often specified at upstream and downstream the valve faces, when sizing and selecting the control valve. Instead of ΔP_{ISA} in Eq. (2), Rahmeyer and Driskell [20] derived Eq. (15) for Δp_{NET} for high recovery valves ($Cv/d^2 > 20$) [21].

$$\frac{Cv_{NET}}{d^2} = \left[\left(\frac{Cv_{ISA}}{d^2}\right)^{-2} - 0.008986 \times f \times \gamma\right]^{-\frac{1}{2}} \quad (15)$$

Cv_{NET} : Cv calculated from ΔP_{NET}
Cv_{ISA} : Cv calculated from ΔP_{ISA}
f : Pipeline friction factor
d: Diameter of the disk in (inches)
γ: Specific gravity of fluid (γ for water = 1)

The difference between ΔP_{NET} and ΔP_{ISA} can be as large as 50% for low and high recovery valves [20]. Small differences in computing the flow coefficient, Cv, and pressure drop can produce significant difference in valve sizing, actuator requirements, and valve cavitation coefficients [22]. Flow coefficient values computed numerically by using ΔP_{NET}, ΔP_{ISA} and Eq. (15) are compared in Fig. 10. The results show that, the relative error between Cv_{ISA} and $Cv_{Manf.}$ has a value of about 50% at 30°, and decreases with increasing the disk angle till reaches 9% at disk angle 90°. There is not enough information about the manufacture valve test benches, and the related standard that was applied. Therefore, the manufacture always should be contacted to verify the valve data. The relative error between numerically calculated Cv_{NET} and Cv_{Rahm} [20] increases with disk angle.

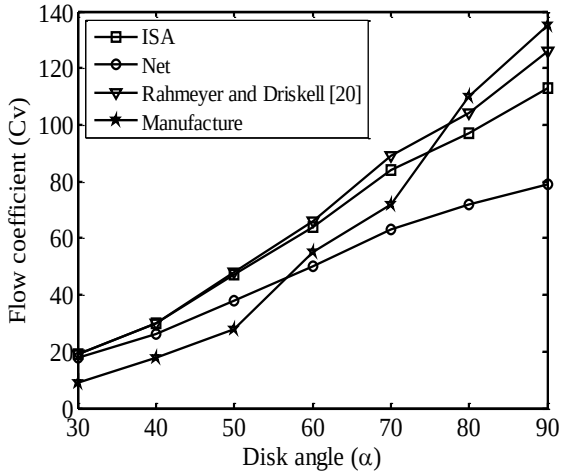

Fig. 10 Valve flow coefficient at different disk angles.

Song and Park [23] found that CFX simulation agreed with the experimental data very well. However, at some positions, especially at the valve opening angle lower than 20°, it didn't agree well. This may be due to the disadvantage of the k-ε turbulence model of its own. Furthermore, it is suggested to use another turbulence model which is good at treatment of near-wall such as the k-ω model and shear stress transport (SST) turbulence model.

5.7 Torque coefficient

The valve actuators are chosen to match the valve closing/opening torques. Torque coefficient is specific for each valve type and geometry. Some valve manufacture tabulated these values with valve disk angle for each valve type. It is difficult for manufacture to determine the exact point for maximum torque and select the right valve actuator to operate the valve automatically. The numerical results of torque coefficient is depicted in Fig. 11, and compared with Henderson el. al. [2]. These results reveal that the maximum value of the torque occurs at disk angle of 70^o. The flow at this position is complex and tends to change over from heavily imbalance to balanced phase.

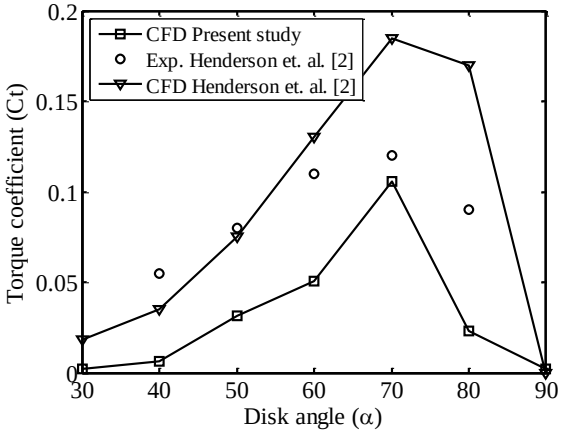

Fig. 11 Valve torque coefficient at different disk angles.

In this study, only torque due to flow (i.e., hydrodynamic) is considered. As discussed in section 5.3 and illustrated in Fig. 7.a for the velocity profile, more

stagnant flow regime is found behind the valve which forms non-uniform pressure distribution and consequently , increases the torque required to open the valve disk further. When these results are compared with the published data OF different authors [2] and manufactures, it was found that the maximum value of the torque occurs at disk angle ranges from 70° to 80° for the butterfly valve. The torque value decreases in the range of 80° to 90° position of the disk because the force distribution on the valve surface is balanced itself [24]. From the comparison between the values of torque coefficient, □□ , with other valve disk styles yields that the disk geometry shape doesn't need any modification to reduce the dynamic torque, as the torque coefficient in these valve styles are less than other valves.

6. Conclusions

The present study shows that the use of CFD tool, such as Fluent 6.3 software, gives good results when analyzing the flow characteristics of butterfly valve. The model yields a good agreement between the experimental data and industrial literatures for the pressure loss, flow, and hydraulic torque coefficients. The results show a formulated relation between the valve disk angle and these coefficients. CFD succeeded to predict the flow coefficient; however, care must be paid at small angles, as the model needs more improvement in itself when applied in the region of high turbulence. Moreover, the results depict that turbulence is small at large angles, and a significant overshoot occurs between disk angles 40° and 50°. Furthermore, the valve Vena contracta moves along diagonal line far away the valve disk with increasing the valve disk angle. The disk hub needs adaption to reduce flow turbulence, in spite of the design is adopted by torque requirement. Therefore, CFD used in valve coefficients calculation introduces a good tool to suggest the need or no need for additional valve modifications.

References

[1] M. Sandalci, E. Mançuhan, E. Alpman, K. Küçükada, Effect of the Flow Conditions and Valve Size on Butterfly Valve Performance, Journal of Thermal Science and Technology, 30(2) (2010) 103-112.

[2] A. Henderson, J. Sargison, G. Walker, J. Haynes, A Numerical Prediction of the Hydrodynamic Torque acting on a Safety Butterfly Valve in a Hydro-electric Power Scheme, WSEAS Transactions on Fluid Mechanics, 3(3) (2008) 218-223.

[3] LLC, Control Valve Handbook, Fisher Control International, 2005.

[4] S.Y. Jeon, J.Y. Yoon, M.S. Shin, Flow Characteristics and Performance Evaluation of Butterfly Valves using Numerical Analysis, 25th IAHR Symposium on Hydraulic Machinery and Systems, IOP Conference Series: Earth and Environmental Science, 12(1) (2010) 012099.

[5] F. Vakili-Tahami, M. Zehsaz, M. Mohammadpour, A. Vakili-Tahami, Analysis of the Hydrodynamic Torque Effects on Large Size Butterfly Valves and Comparing Results with AWWA C504 Standard Recommendations, Journal of Mechanical Science and Technology, 26(9) (2012) 2799-2806.

[6] K. Thanigavelmurugan, N.V. Mahalakshmi, S.M. Das, D. Venkatesh, Performance Improvement of a Control Valve using Computational Fluid Dynamics, Proceedings of the National Conference on Trends and Advances in Mechanical Engineering, YMCA University of Science & Technology, Faridabad, Haryana, India, 2012 , 106-113.

[7] Z. Leutwyler, C. Dalton, A CFD Study to Analyze the Aerodynamic Torque, Lift, and Drag Forces for a Butterfly Valve in the Mid-Stroke Position, ASME 2004 Heat Transfer/Fluids Engineering Summer Conference, Charlotte, North Carolina, USA, 2004, Paper HT-FED04-56016.

[8] N.T. Shirazi, G.R. Azizyan, G.H. Akbari, CFD Analysis of the Ball Valve

Performance in Presence of Cavitation, Life Science Journal, 9(4) (2012) 1460-1467.

[9] V.J. Sonawane, T.J. Rane, A.D. Monde, R.V. Vajarinkar, P.C. Gawade, Design and Analysis of Globe Valve as Control Valve Using CFD Software, Second National Conference on Recent Developments in Mechanical Engineering, M.E.Society's College of Engineering, Wadia College Campus, Pune, India, 2013 , pp. 63-71.

[10] L. Wang, X. Song, Y. Park, The Improvement of Large Butterfly Valve by Using Numerical Analysis Method, Proceedings of the 6th WSEAS International Conference on Fluid Mechanics (FLUIDS'09), Vouliagmeni, Athens, Greece, 2009, 75-79.

[11] T.N. Price, Transient Effects on Dynamic Torque for Butterfly Valves, M.Sc.thesis, Utah State University, Logan, Utah ,USA, 2013.

[12] R. Morita, F. Inada, M. Mori, K. Tezuka, Y. Tsujimoto, CFD Calculation and Experiments of Unsteady Flow on Control Valve, ASME 2004 Heat Transfer/Fluids Engineering Summer Conference, Charlotte, North Carolina, USA, 2004, Paper HT-FED04-56017.

[13] B. Prema, S. Bhojani, N. Gopalakrishnan, Design Optimization of Butterfly Valve using CFD,Proceedings of the 37th National & 4th International Conference on Fluid Mechanics and Fluid Power, IIT Madras, Chennai, India, 2010, Paper, FMFP10-FP-15.

[14] M.-J. Chern, C.-C. Wang, Control of Volumetric Flow-Rate of Ball Valve Using V-Port, Journal of Fluids Engineering, 126(3) (2004) 471-481.

[15] AWWA, Butterfly Valves: Torque, Head Loss, and Cavitation Analysis, Manual of Water Supply Practices - M49, American Water Works Association, 2012.

[16] ANSI/ISA, Flow of Fluids through Valves, Fittings, and Pipe, CRANE (Ed.) Control Valve Capacity Test Procedures: Ansi/Isa-S75.02-1996, ISA, 1996.

[17] C. Huang, R.H. Kim, Three-Dimensional Analysis of Partially Open Butterfly Valve Flows, Journal of Fluids Engineering, 118(3) (1996) 562-568.

[18] D.F. Young, B.R. Munson, T.H. Okiishi, A Brief Introduction to Fluid Mechanics, Wiley, 2004.

[19] G. Ibrahim, Z. Al-Otaibi, H.M. Ahmed, An Investigation of Butterfly Valve Flow Characteristics Using Numerical Technique, Journal of Advanced Science and Engineering Research, 3(2) (2013) 151-166.

[20] W. Rahmeyer, L. Driskell, Control Valve Flow Coefficients, Journal of Transportation Engineering, 111(4) (1985) 358-364.

[21] J.W. Hutchison, ISA Handbook of Control Valves, 2 ed., Instrument Society of America, Pittsburgh, USA, 1976.

[22] ISA, ISA Standards, Recommended Practice and Technical Reports, Control Valves, ISA, USA, 1999.

[23] X.G. Song, Y.C. Park, Numerical Analysis of Butterfly Valve-Prediction of Flow Coefficient and Hydrodynamic Torque Coefficient, Proceedings of the World Congress on Engineering and Computer Science, WCECS 2007, San Francisco, USA, 2007.

[24] W. Chaiworapuek, The Engineering Investigation of the Water Flow past the Butterfly Valve, Institut National des Sciences Appliquées de Lyon, France, 2007.